Beam Size Measurement

- Survey of beam size measurement techniques and applications.
- Detailed analysis of an X-Ray pinhole camera
  - Description
  - What is actually measured?
  - Image processing and resolution

Gaussian beam profile

- Electrons in storage ring damp to 2D Gaussian distribution.

$$A_0 \exp\left(-\frac{\beta x'^2 + 2\alpha x x' + \gamma x^2}{2\varepsilon}\right)$$

$$\sigma_x = \sqrt{\beta_x \varepsilon_x}$$

$$\sigma_x' = \sqrt{\gamma_x \varepsilon_x}$$

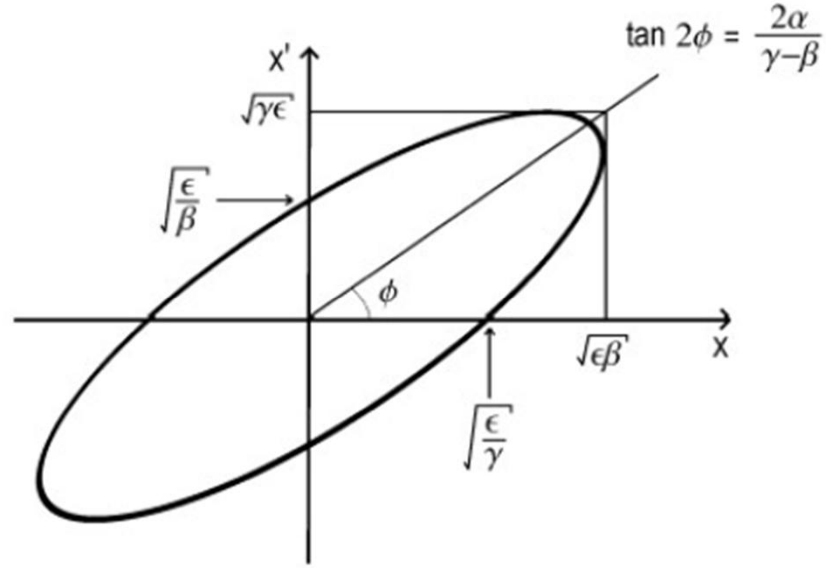

- Similar distribution in y.

Beam size measurements

X-Ray pinhole camera

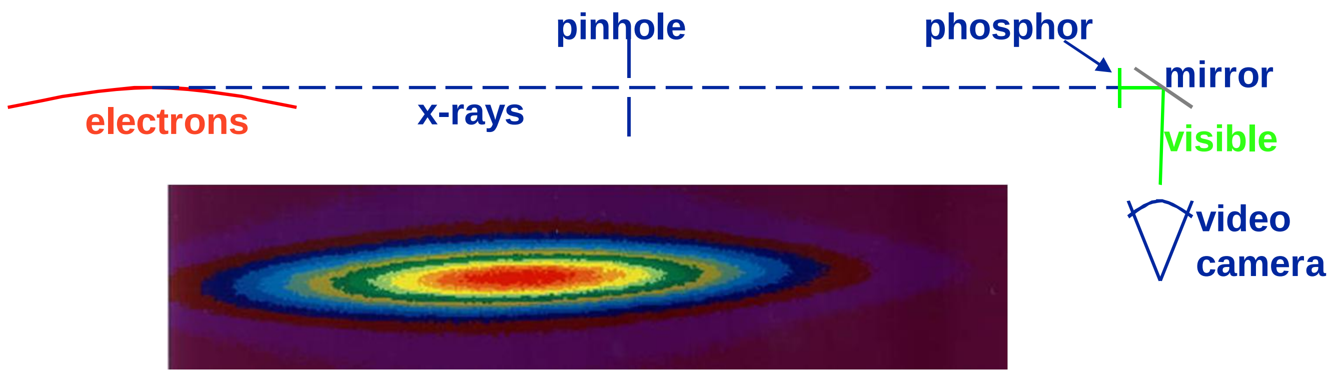

Pinhole camera array

(Kuske et al., Bessy)

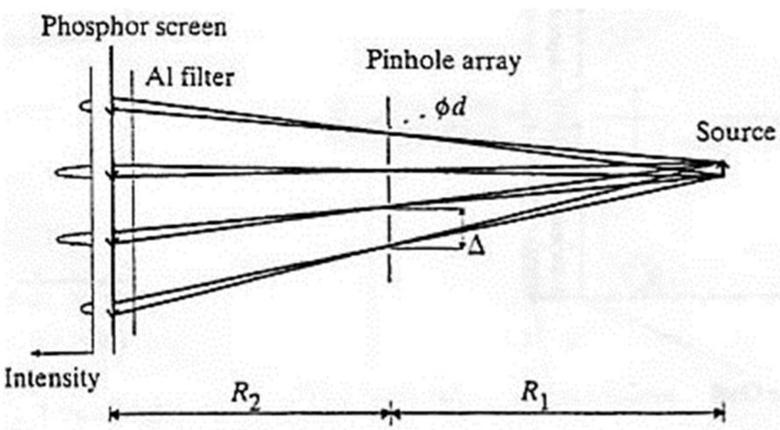

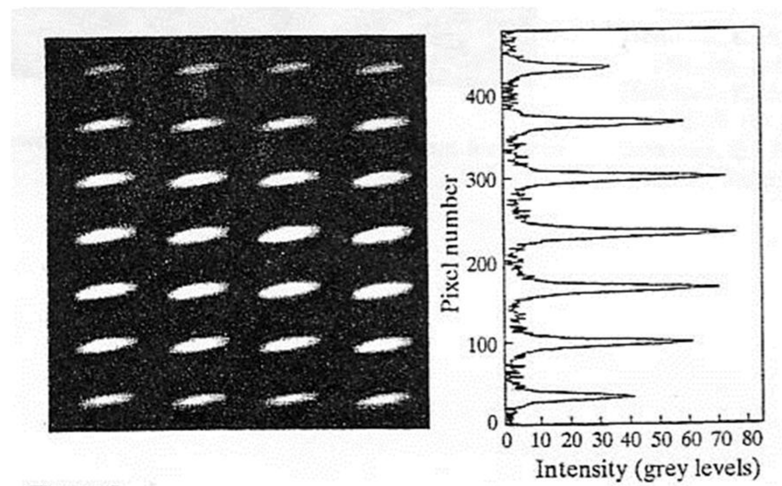

Figure 2
Left: image of a portion of the phosphor observed on a BESSY I bending magnet. Right: integrated intensities of one column of images on the phosphor.

Turn-by-turn monitor

Turn-by-turn measurements of synchrotron radiation are used for measuring beam instability and injection mis-match.

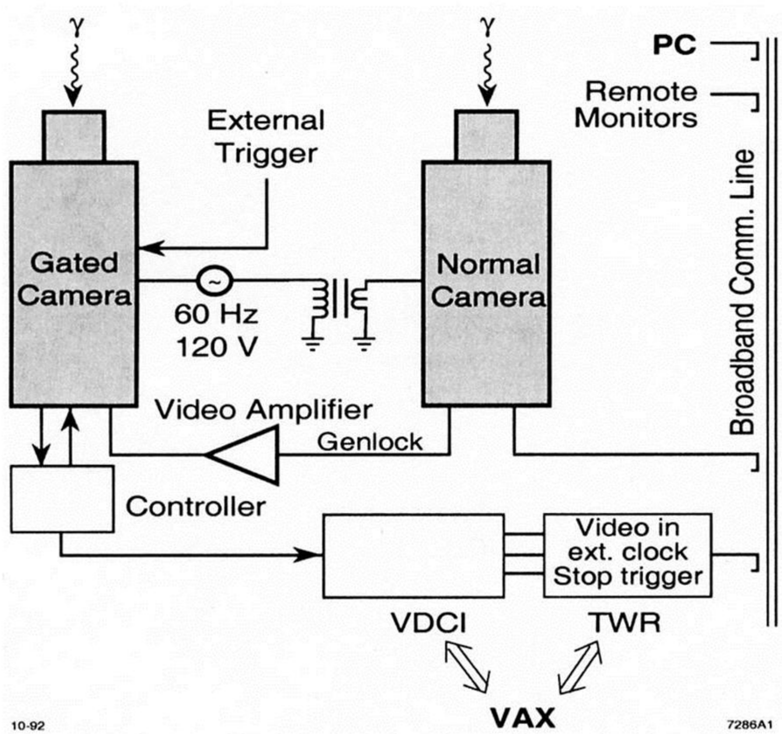

Minty and Spence, PAC'95

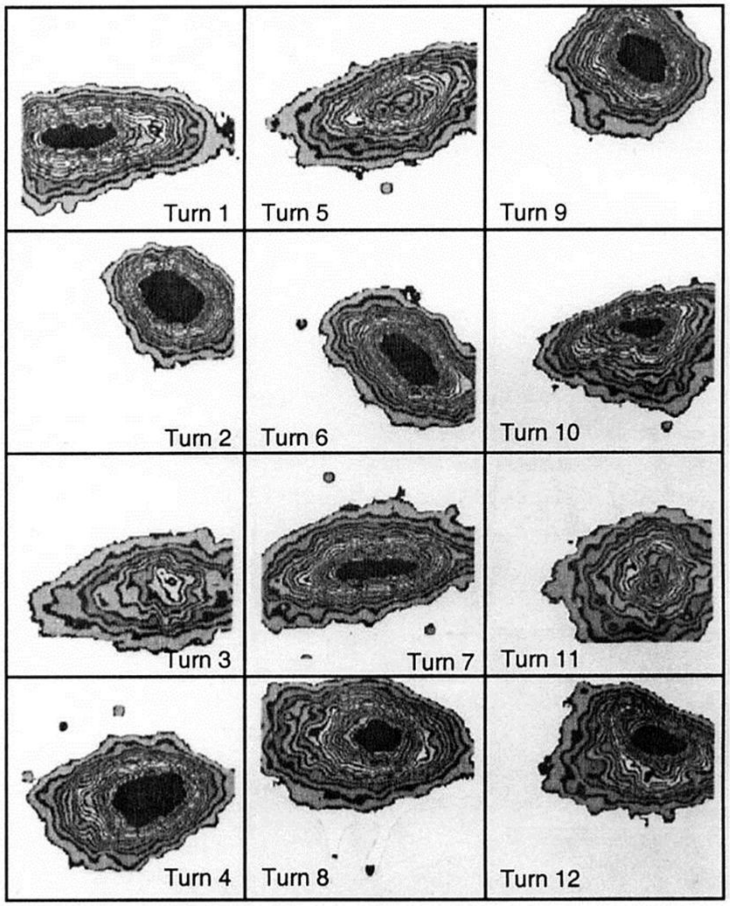

Beam size measurement, spatial coherence
(Mitsuhashi, PAC97)

Michelson's method for measuring the size of stars applied to measuring electron beam size. Spatial cohence increases as beam size decreases.

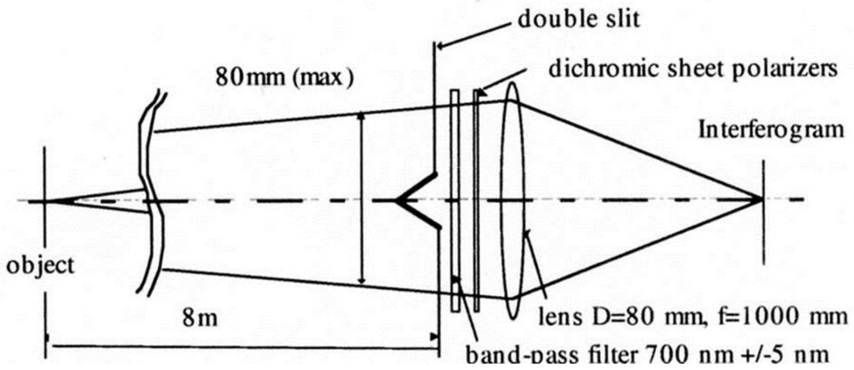

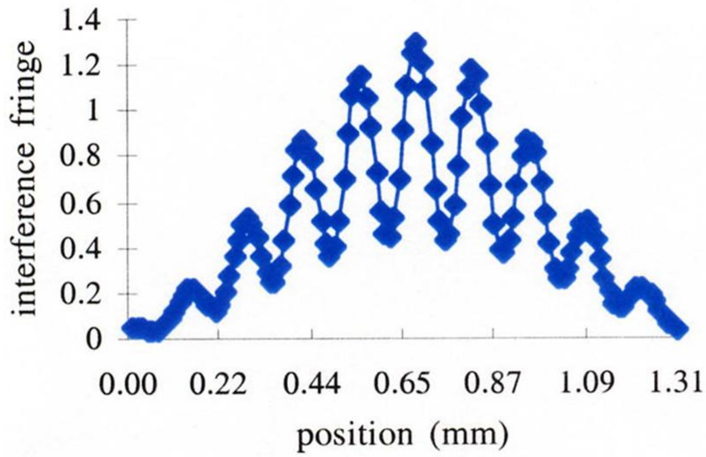

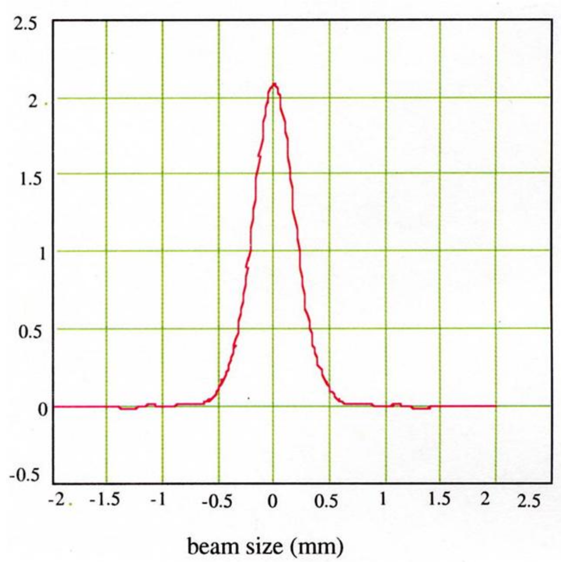

← **Vertical beam size can be obtained from the Fourier transform of the degree of spatial coherence.**

2D visible light interferometer

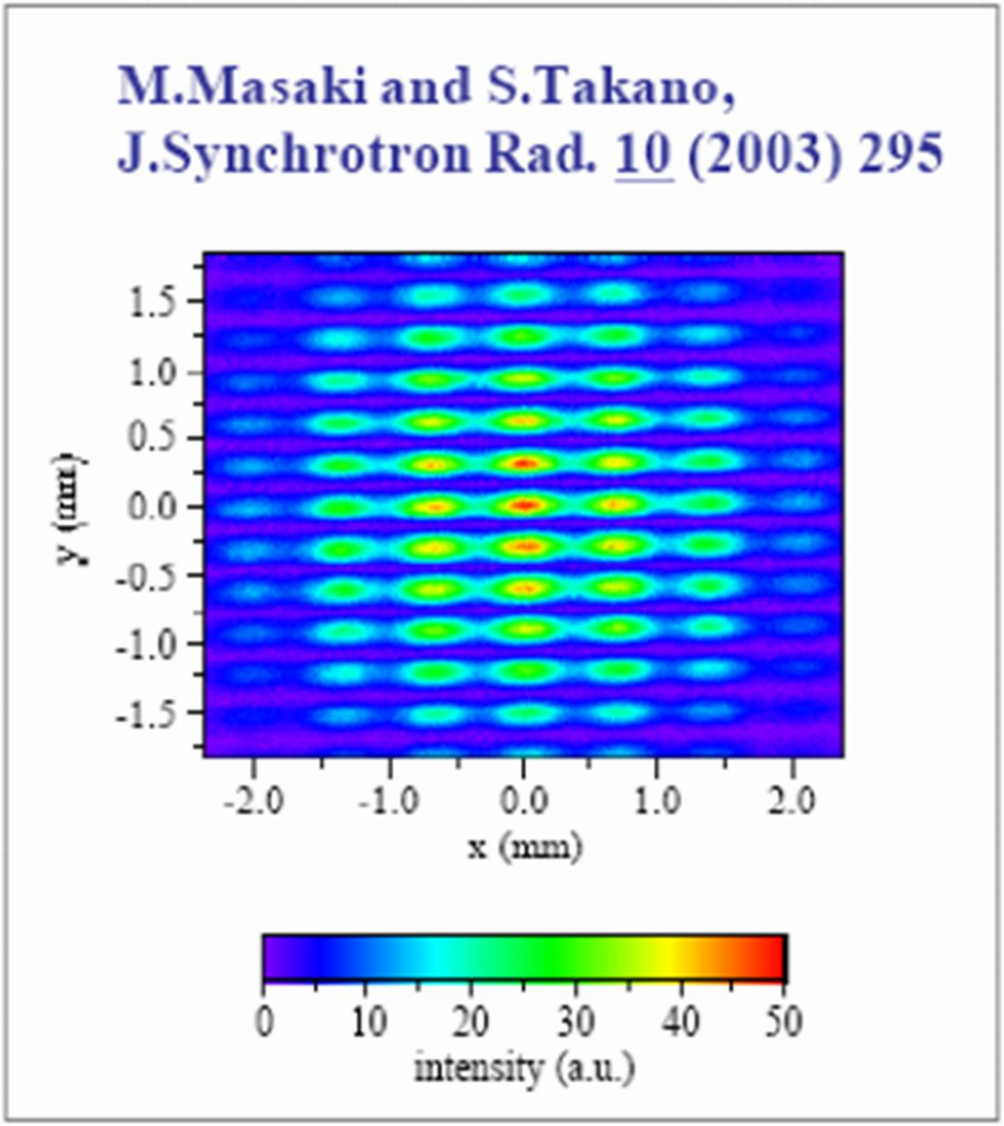

π-mode SR beam size measurement

- Image vertically polarized SR
- Intensity at y=0 determined by ε_y
- Andersson et al., NIMA 591 (2008).
- Angela Saa Hernandez, ALERT 2014 Workshop

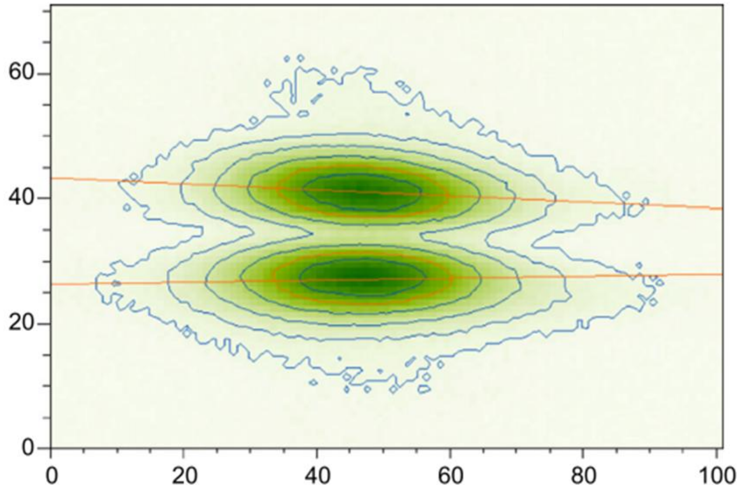

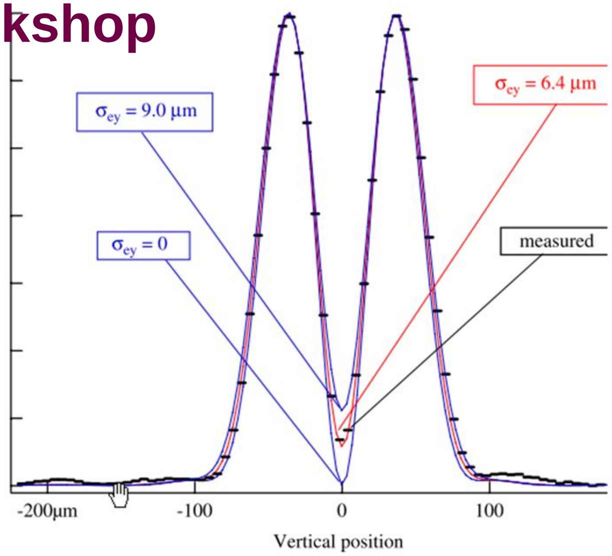

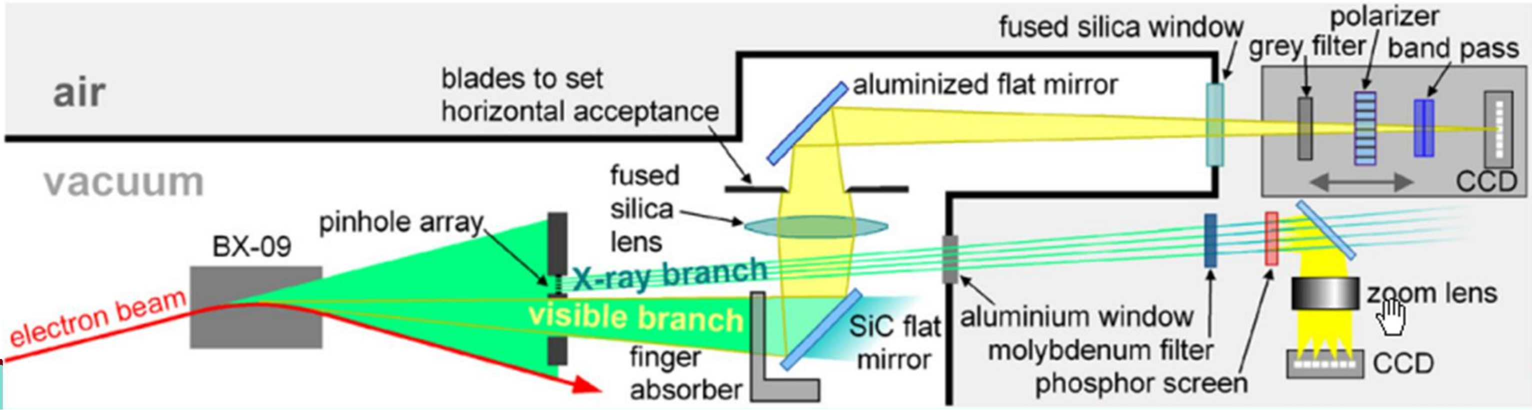

Vertical emittance measurement in Australia with vertical undulator

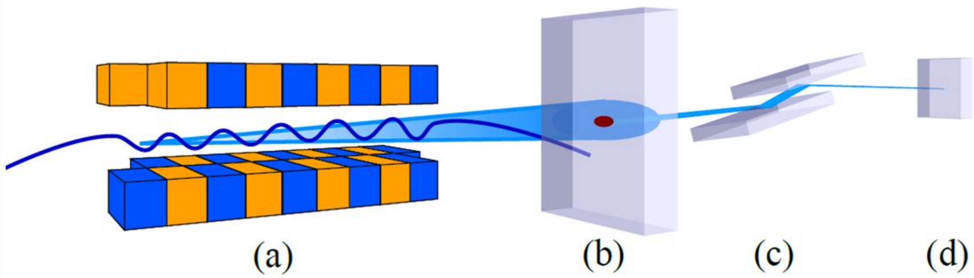

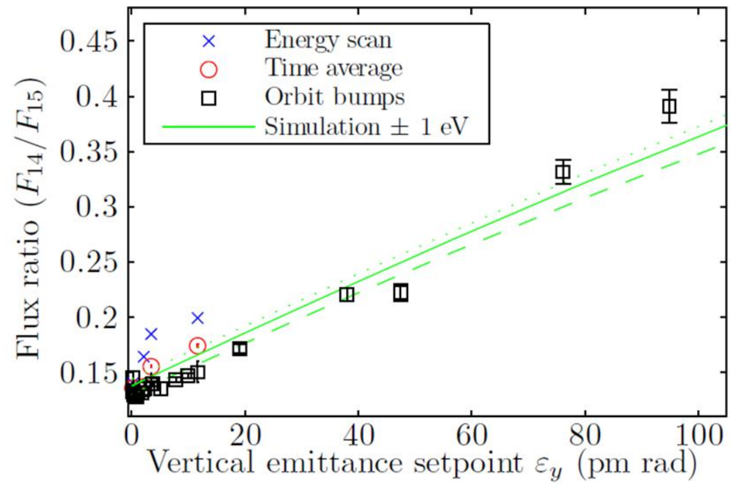

6th harmonic, pm rad emittance

Measured

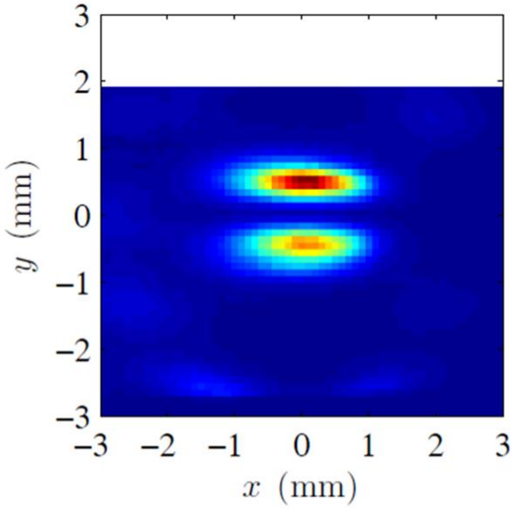

Simulation

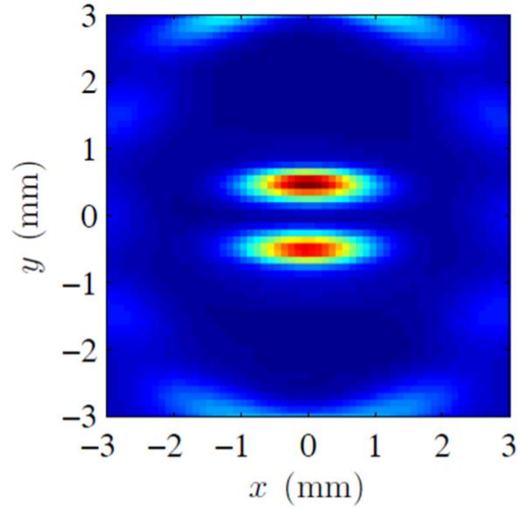

- **Useful pm rad emittance monitor**
- **Non-Gaussian radiation distribution**

Kent Wootton, thesis (2014): http://hdl.handle.net/11343/39616

Beam size measurements

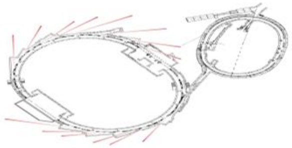

Touschek lifetime

$$\tau_{T_{1/2}} \propto \text{bunch volume}$$

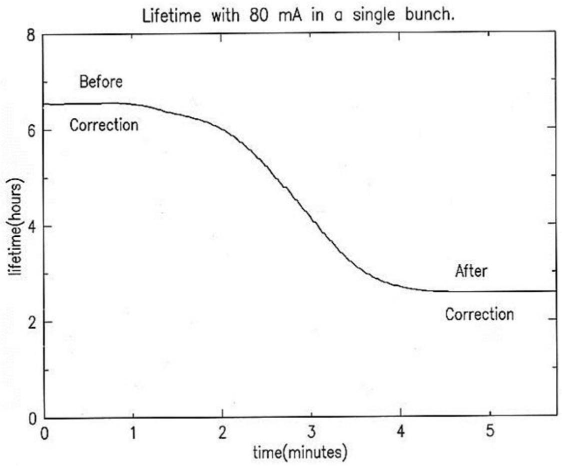

Scrapers measure beam halo

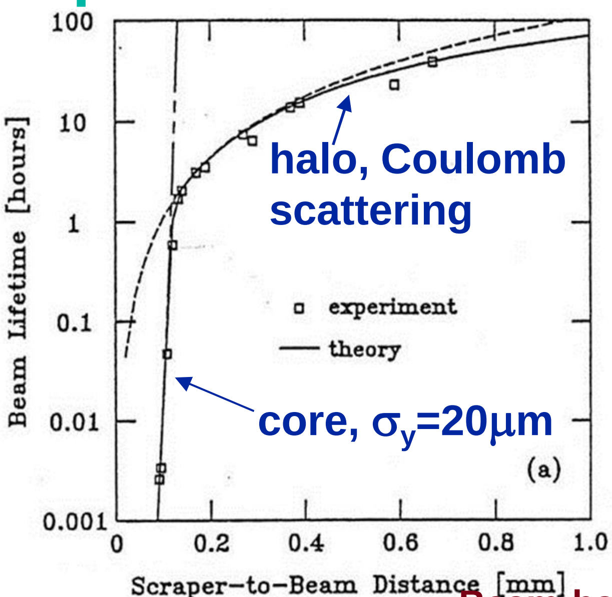

Peter Stefan et al., NIMA, 1998

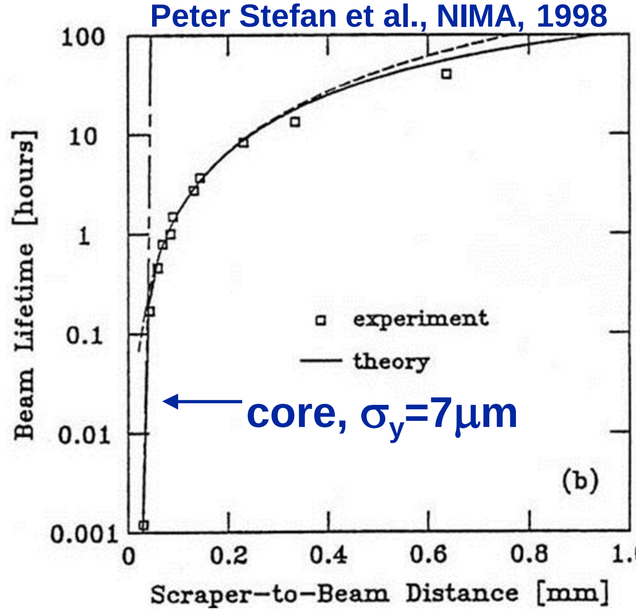

Laser wire beam size measurement

A laser wire successfully measured very small beam sizes at KEK ATF, H. Sakai et al., PRST-AB Volume 5 (2002)

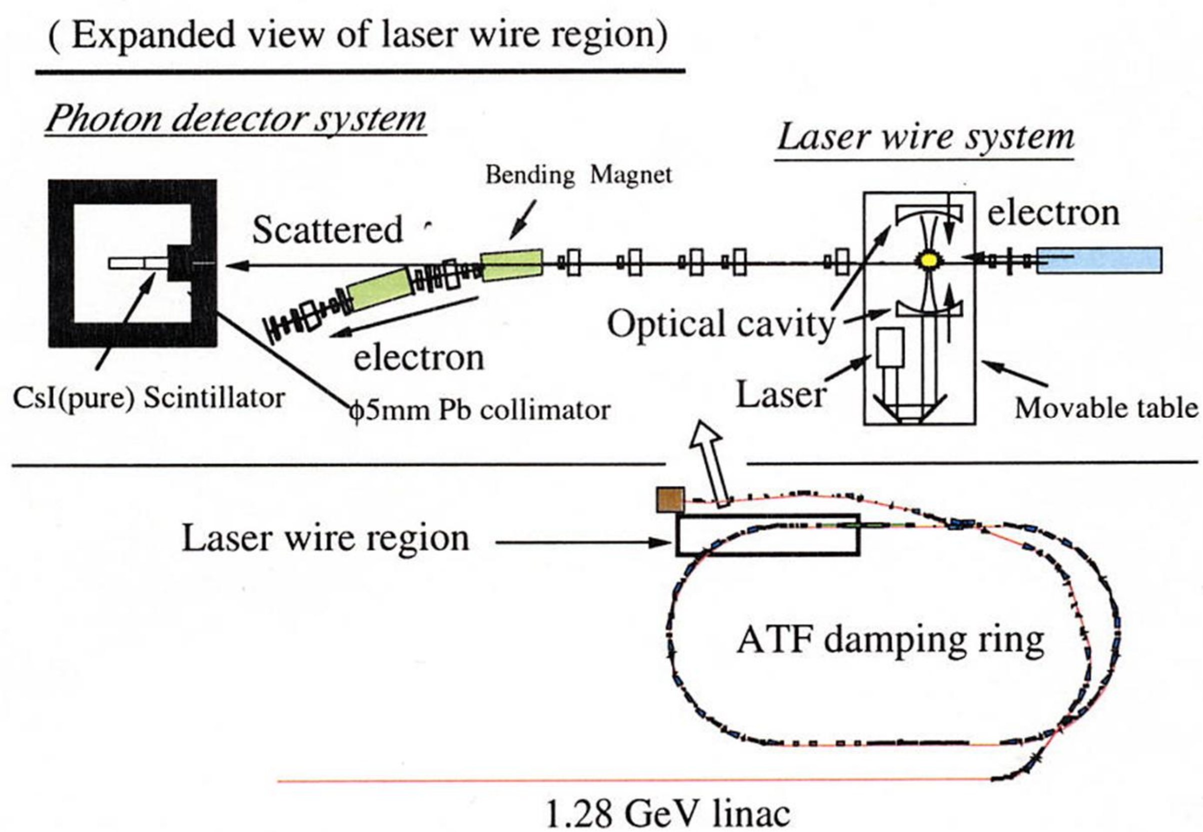

Measures of beam size

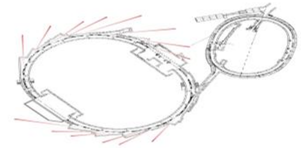

❍**Luminosity scan** **(Y. Cai, EPAC'00, p 400)**

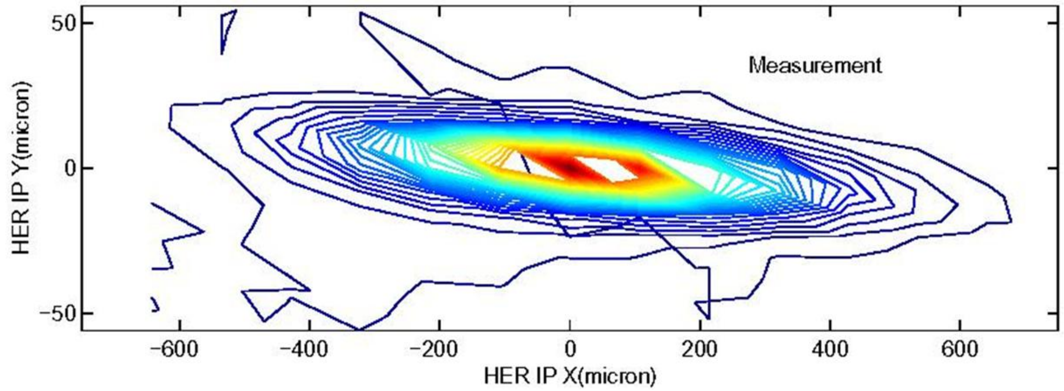

❍**Beam-beam scan,** **(Wenninger et al., EPAC98)**

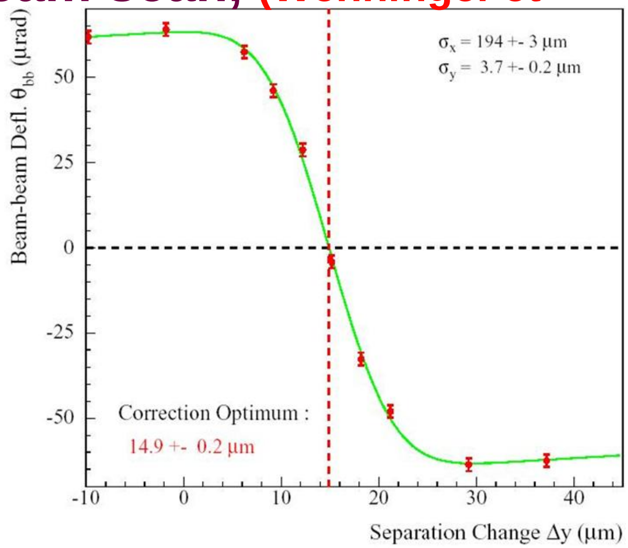

❍**Quadrupole moment detectors**
(A. Jansson et al., CERN-PS, PAC'99)

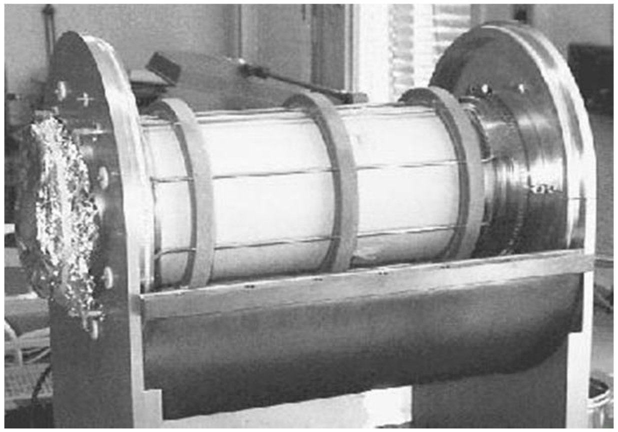

Measurement of the Transverse Beam Emittance

Method I: quadrupole scan

Principle: with a well-centered beam, measure the beam size as a function of the quadrupole field strength

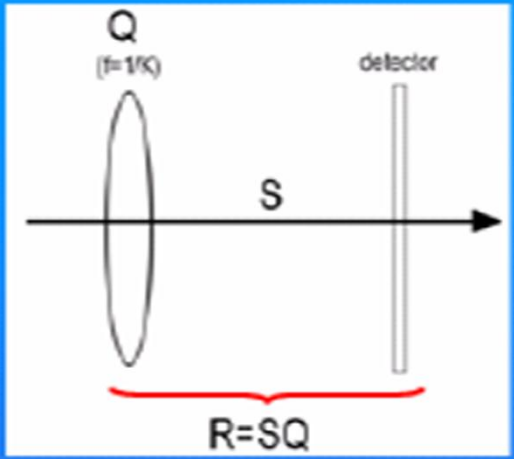

Here
Q is the transfer matrix of the quadrupole
R is the transfer matrix between the quadrupole and the beam size detector

With $Q = \begin{pmatrix} 1 & 0 \\ K & 1 \end{pmatrix}$ then $R = \begin{pmatrix} S_{11} + KS_{12} & S_{12} \\ S_{21} + KS_{22} & S_{22} \end{pmatrix}$ with $\Sigma_{\text{beam}} = R\Sigma_{\text{beam},0}R^t$

The (11)-element of the beam transfer matrix is found after algebra to be:

$$\Sigma_{11}(= \langle x^2 \rangle) = ({S_{11}}^2 \Sigma_{11_0} + 2S_{11}S_{12}\Sigma_{12_0} + {S_{12}}^2\Sigma_{22_0}) + (2S_{11}S_{12}\Sigma_{11_0} + 2{S_{12}}^2\Sigma_{12_0})K + {S_{12}}^2\Sigma_{11_0}K^2$$

which is quadratic in the field strength, K

M. Minty, F. Zimmermann

Measurement: measure beam size versus quadrupole field strength

recall:

$$\Sigma_{11}(=\langle x^2\rangle) = ({S_{11}}^2\Sigma_{11_o} + 2S_{11}S_{12}\Sigma_{12_o} + {S_{12}}^2\Sigma_{22_o}) + (2S_{11}S_{12}\Sigma_{11_o} + 2{S_{12}}^2\Sigma_{12_o})K + {S_{12}}^2\Sigma_{11_o}K^2$$

data:

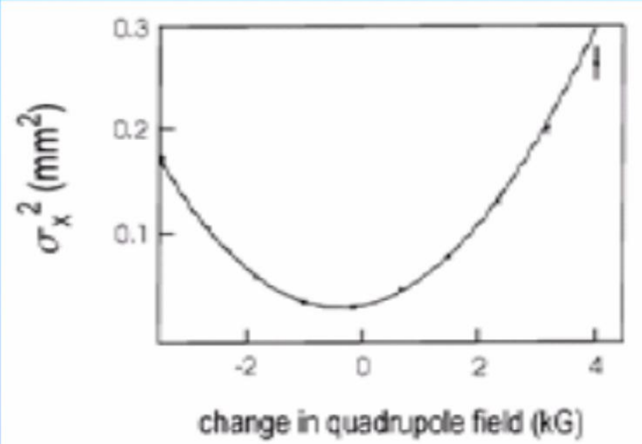

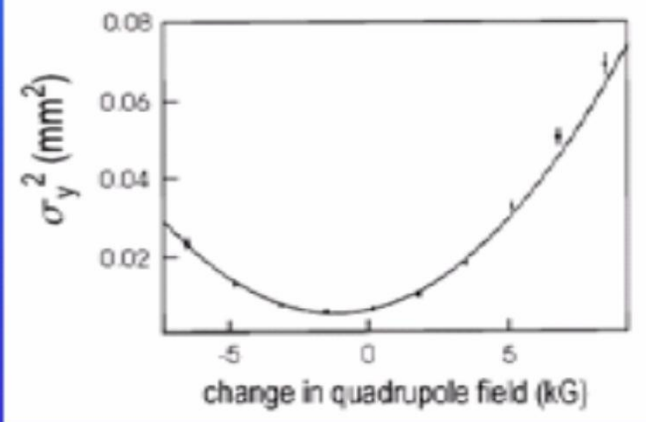

fitting function (parabolic):

$$\begin{aligned}\Sigma_{11} &= A(K-B)^2 + C \\ &= AK^2 - 2ABK + (C + AB^2)\end{aligned}$$

equating terms (drop subscripts 'o'),

$$A = S_{12}^2\Sigma_{11}\,,$$

$$-2AB = 2S_{11}S_{12}\Sigma_{11} + 2S_{12}^2\Sigma_{12}\,,$$

$$C + AB^2 = {S_{11}}^2\Sigma_{11} + 2S_{11}S_{12}\Sigma_{12} + {S_{12}}^2\Sigma_{22}$$

solving for the beam matrix elements:

$$\Sigma_{11} = A/{S_{12}}^2\,,$$

$$\Sigma_{12} = -\frac{A}{{S_{12}}^2}\left(B + \frac{S_{11}}{S_{12}}\right)\,,$$

$$\Sigma_{22} = \frac{1}{{S_{12}}^2}\left[(AB^2 + C) + 2AB\left(\frac{S_{11}}{S_{12}}\right) + A\left(\frac{S_{11}}{S_{12}}\right)^2\right]$$

M. Minty, F. Zimmermann

Determining ε_y from measured <y^2>

- ESRF – many beam size diagnostics
- See differing σ^2_y/β_y at each location
- For details, see Christoph's coupling lecture
- A. Franchi et al., PRST-AB-14-012804 (2011).

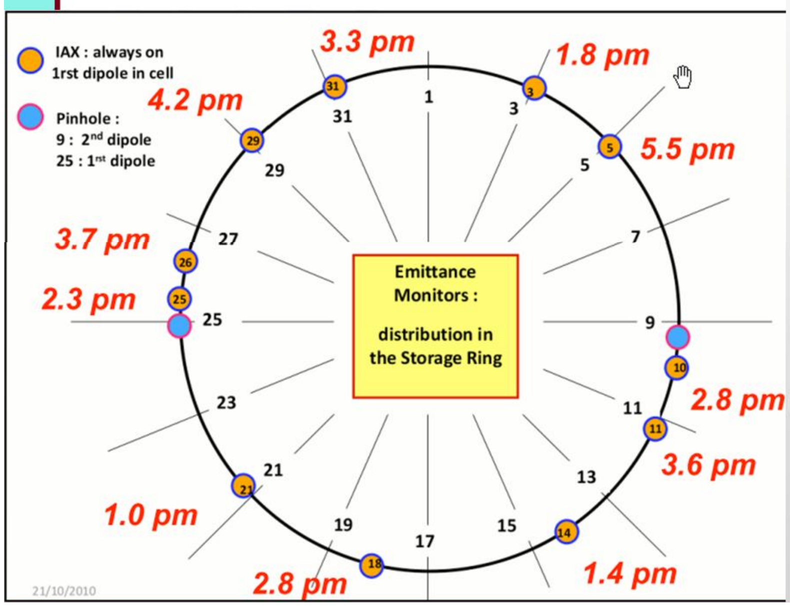

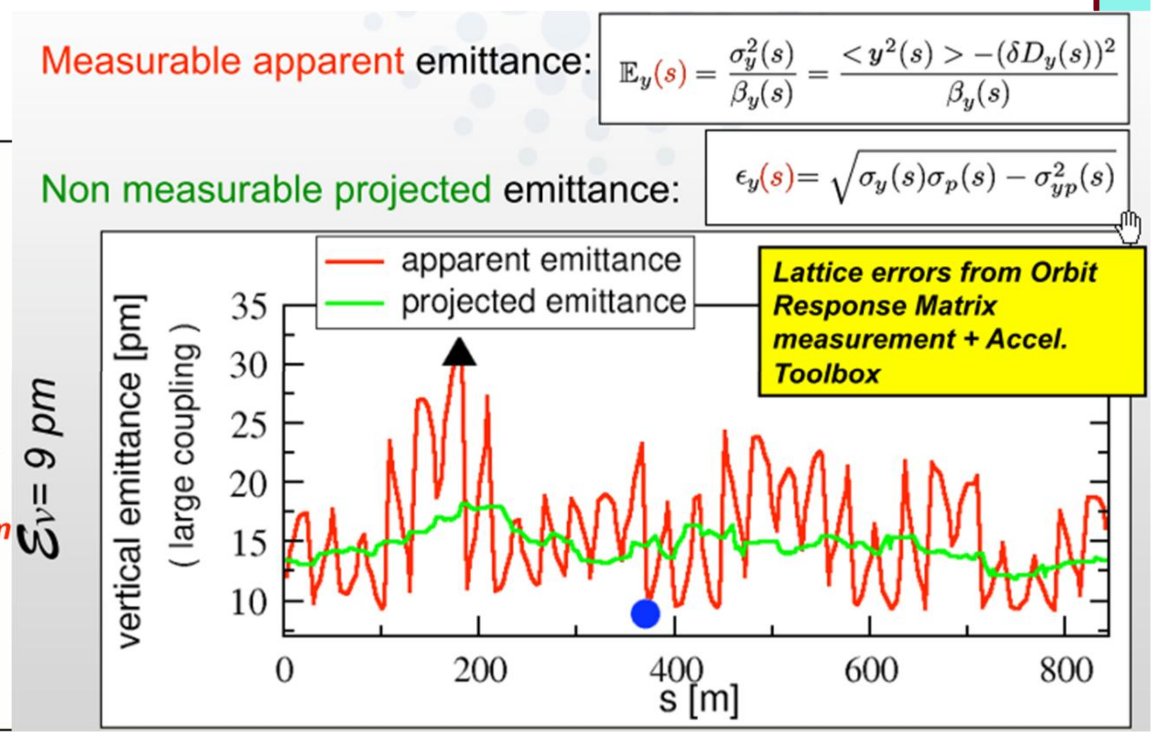

X-Ray pinhole camera

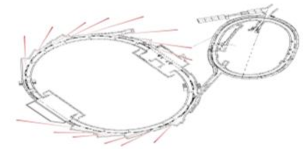

Pinhole camera on X28 dipole beamline at NSLS X-Ray Ring:

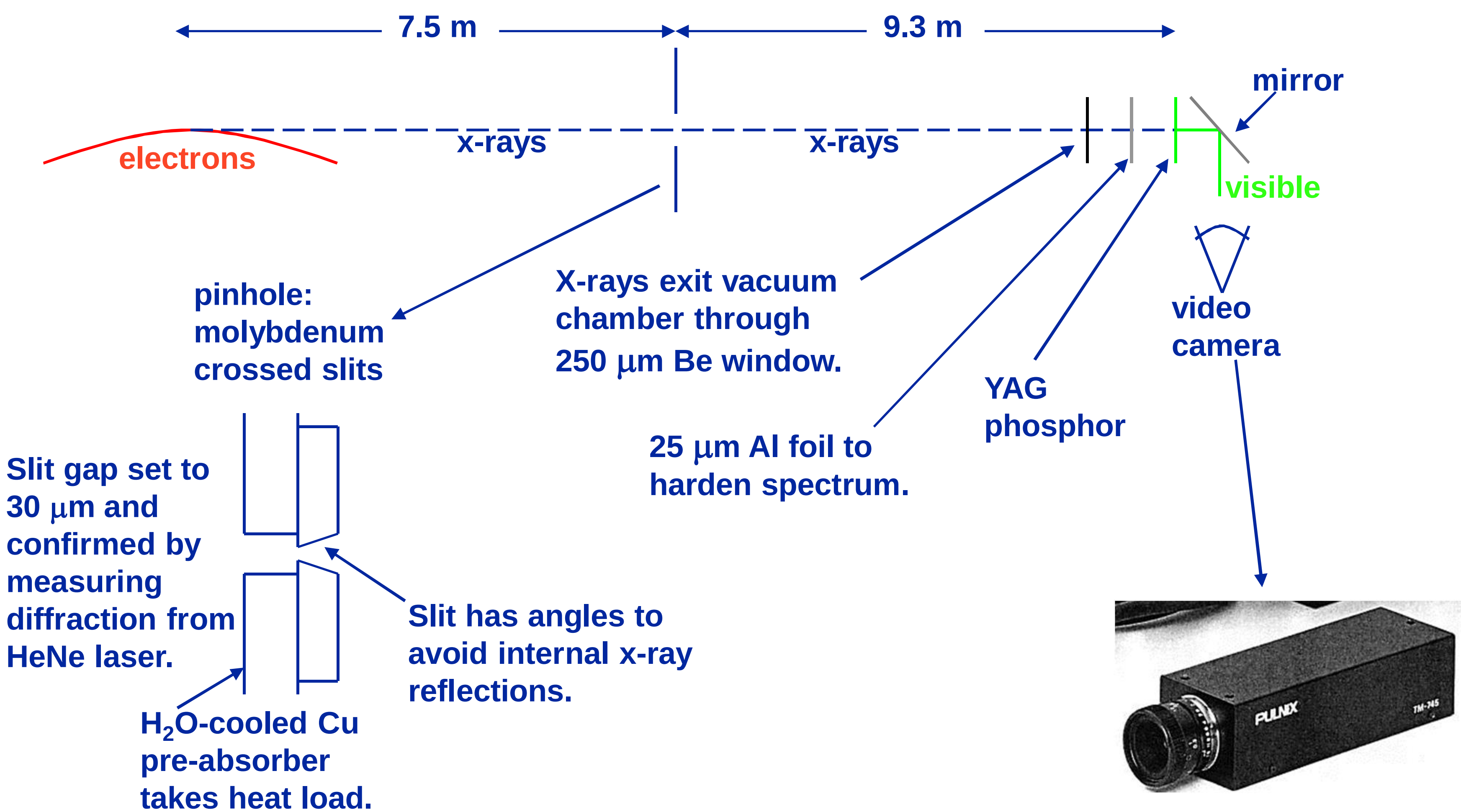

What is measured?

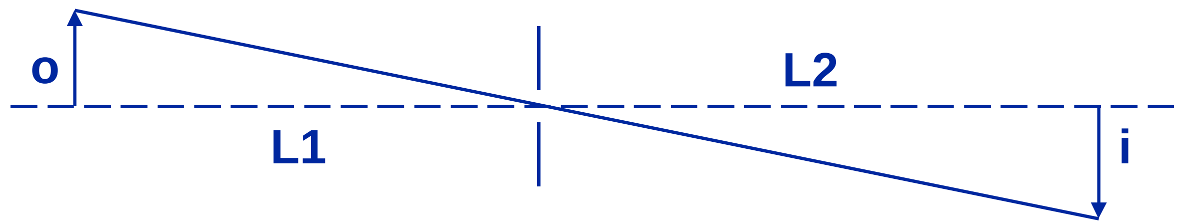

The standard formula for a pinhole camera, i=(L2/L1)o, assumes that the object is radiating light equally in all directions. Synchrotron radiation is highly collimated in the direction of the electrons, so this formula does not necessarily hold.

I’ll show that for a dipole beamline, it does hold in the horizontal plane, but does not in general in the vertical plane.

The problem in the vertical plane is that electrons at the top of “o” (in this case the top of the electron beam) do not necessarily radiate photons that go through the pinhole, so i<(L2/L1)o.

Review of electron phase space

The on-energy electrons in a storage ring make a Gaussian in phase space. Area of e$^{-1/2}$ ellipse is ε.

$$\exp\left(-\frac{\gamma x^2 + 2\alpha x x' + \beta x'^2}{2\epsilon}\right)$$

$$\alpha = -\frac{\beta'(s)}{2}, \qquad \gamma = \frac{1+\alpha^2}{\beta}$$

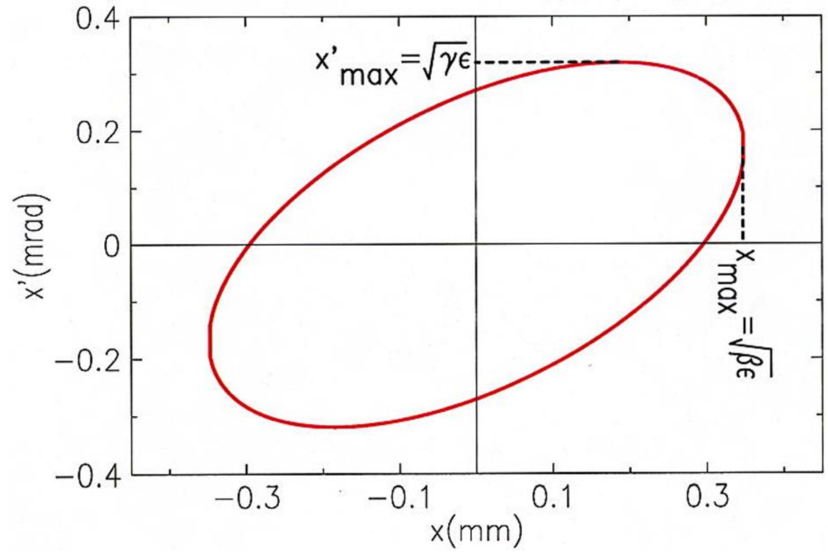

The full extent of the electron beam including energy spread is larger.

$$\bar{\epsilon} = \epsilon\bar{\kappa}, \qquad \bar{\alpha} = \frac{\alpha - \frac{\eta\eta'\sigma_\delta^2}{\epsilon}}{\bar{\kappa}}$$

$$\bar{\beta} = \frac{\beta + \frac{\eta^2\sigma_\delta^2}{\epsilon}}{\bar{\kappa}}, \qquad \bar{\gamma} = \frac{\gamma + \frac{\eta'^2\sigma_\delta^2}{\epsilon}}{\bar{\kappa}}$$

$$\bar{\kappa} \equiv \sqrt{1 + \frac{\sigma_\delta^2}{\epsilon}(\gamma\eta^2 + 2\alpha\eta\eta' + \beta\eta'^2)}.$$

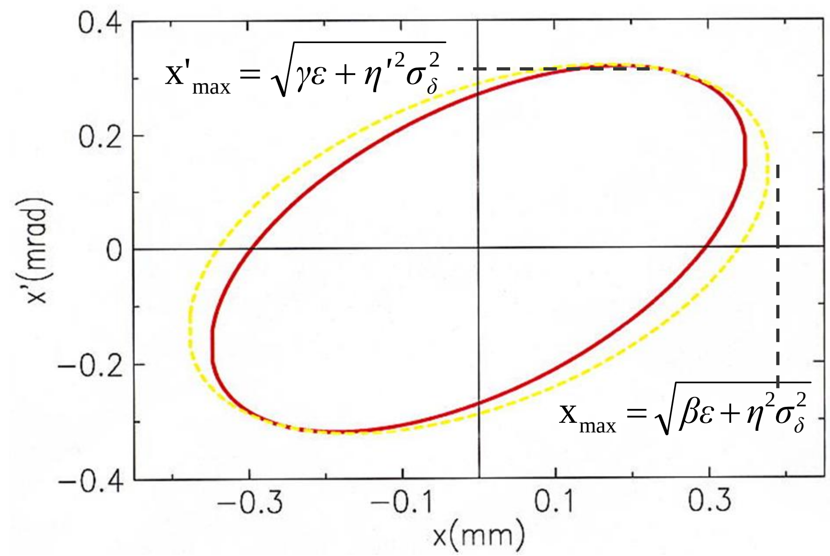

Phase space distribution of photons at source

photon ellipse at source point

Full e- ellipse with energy spread

on-energy e-

Start with on-energy electron ellipse

$$\exp\left(-\frac{\gamma x^2 + 2\alpha x x' + \beta x'^2}{2\epsilon}\right)$$

Add energy spread, σ_δ

$$\otimes$$

$$\exp\left(-\frac{x^2}{2\eta^2\sigma_\delta^2}\right)\delta(\eta' x - \eta x')$$

Add photon opening angle, $\sigma_{r'} = \frac{.565}{\gamma_0}\left(\frac{E_c}{E}\right)^{.425}$

$$\otimes$$

$$\exp\left(-\frac{x'^2}{2\sigma_{r'}^2}\right)\delta(x)$$

$$\sigma_r = \frac{\lambda}{4\pi\sigma'_r} \approx 0$$

Photon ellipse at source

$$\epsilon_p = \epsilon\kappa, \qquad \alpha_p = \frac{\alpha - \frac{\eta\eta'\sigma_\delta^2}{\epsilon}}{\kappa}$$

$$\beta_p = \frac{\beta + \frac{\eta^2\sigma_\delta^2}{\epsilon}}{\kappa}, \qquad \gamma_p = \frac{\gamma + \frac{\eta'^2\sigma_\delta^2 + \sigma_{r'}^2}{\epsilon}}{\kappa}$$

$$\kappa \equiv \sqrt{1 + \frac{\sigma_\delta^2}{\epsilon}(\gamma\eta^2 + 2\alpha\eta\eta' + \beta\eta'^2) + \frac{\beta\sigma_{r'}^2}{\epsilon} + \frac{\eta^2\sigma_\delta^2\sigma_{r'}^2}{\epsilon^2}}.$$

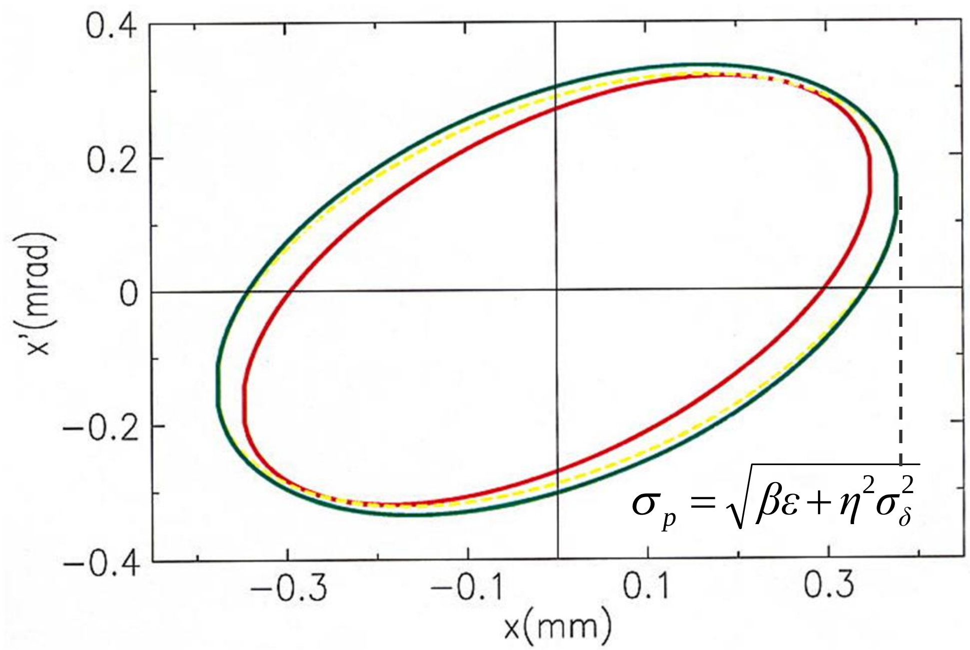

on energy electrons

electrons including energy spread

photons

Measured vertical profile

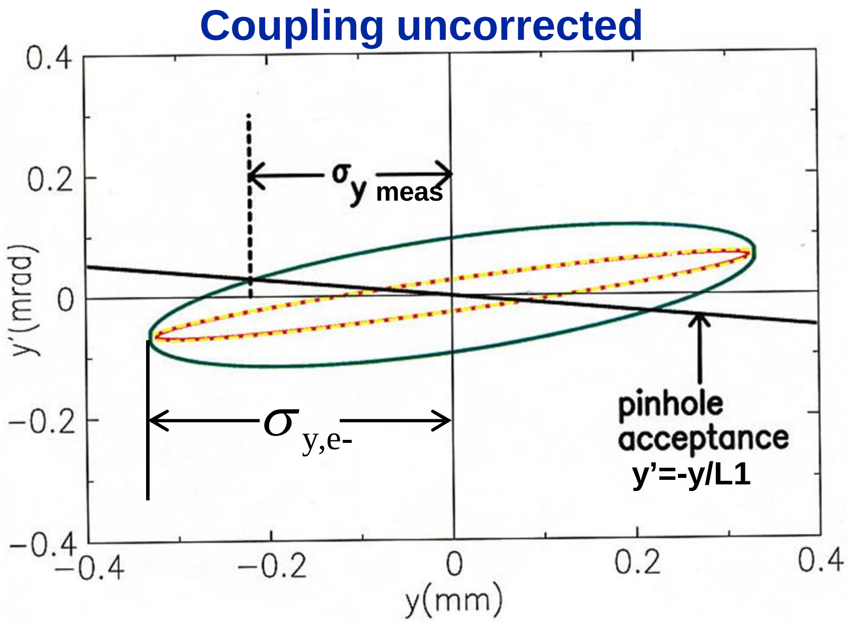

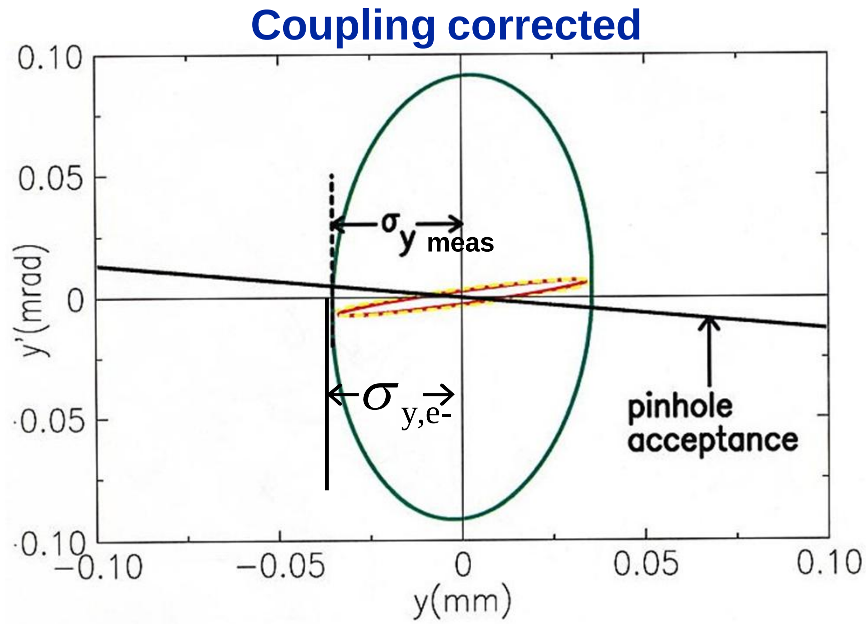

The beam profile at the source point seen by the pinhole camera is the intersection of the pinhole camera acceptance, y'=-y/L1, and the photon ellipse. $\sigma_{\mathrm{y,meas}} \neq \sigma_{\mathrm{y,e-}}$ **The electron emittance can be found with:**

$$\varepsilon^2 + B\varepsilon + C = 0$$

$$B = -\sigma^2_{\mathrm{y,meas}}(\gamma - 2\alpha/L1 + \beta/L1^2) + \sigma^2_\delta(\gamma\eta^2 + 2\alpha\eta\eta' + \beta\eta'^2) + \beta\sigma^2_{r'}$$

$$C = -\sigma^2_{\mathrm{y,meas}}(\sigma^2_{r'} + \sigma^2_\delta(\eta' + \eta/L1)^2) + \eta^2\sigma^2_\delta\sigma^2_{r'}$$

Measured horizontal profile

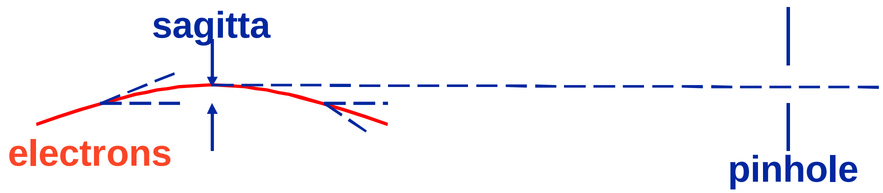

The ellipse sweeps across the pinhole acceptance in an arc in (x,x'). The sagitta (the change in x) is negligibly small.

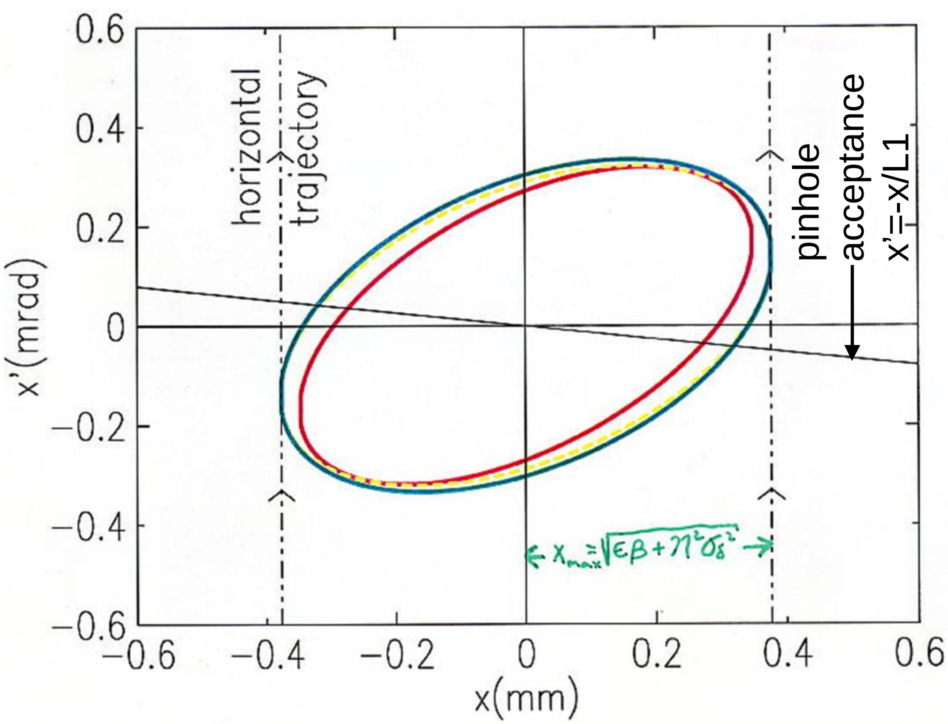

In the fixed coordinates at the beamline source point, the photon ellipse sweeps across the pinhole acceptance. Integrating the changing profile gives:

$$\int_{-\infty}^{+\infty} dx'_0\, e^{-\left(\frac{\gamma_p x^2+2\alpha_p x x'(x,x'_0)+\beta_p x'^2(x,x'_0)}{2\epsilon_p}\right)},$$

$$x'(x,x'_0) = x'_0 - x/L1.$$

which gives

$$\exp\left(-\frac{x^2}{2(\epsilon\beta+\eta^2\sigma_\delta^2)}\right).$$

The integrated profile seen by the pinhole camera is

$$\sigma_{x,\text{meas}} = \sqrt{\varepsilon\beta+\eta^2\sigma_\delta^2} = \sigma_{x,e-}$$

Resolution & image processing

Two contributions to resolution:

1. Pinhole diffraction.
2. Resolution of detector (phosphor, mirror, lens, and CCD).

The two resolution functions are deconvolved from each horizontal and vertical slice. A two dimensional, tilted Gaussian is fit to the resulting profile.

Example for one vertical slice.

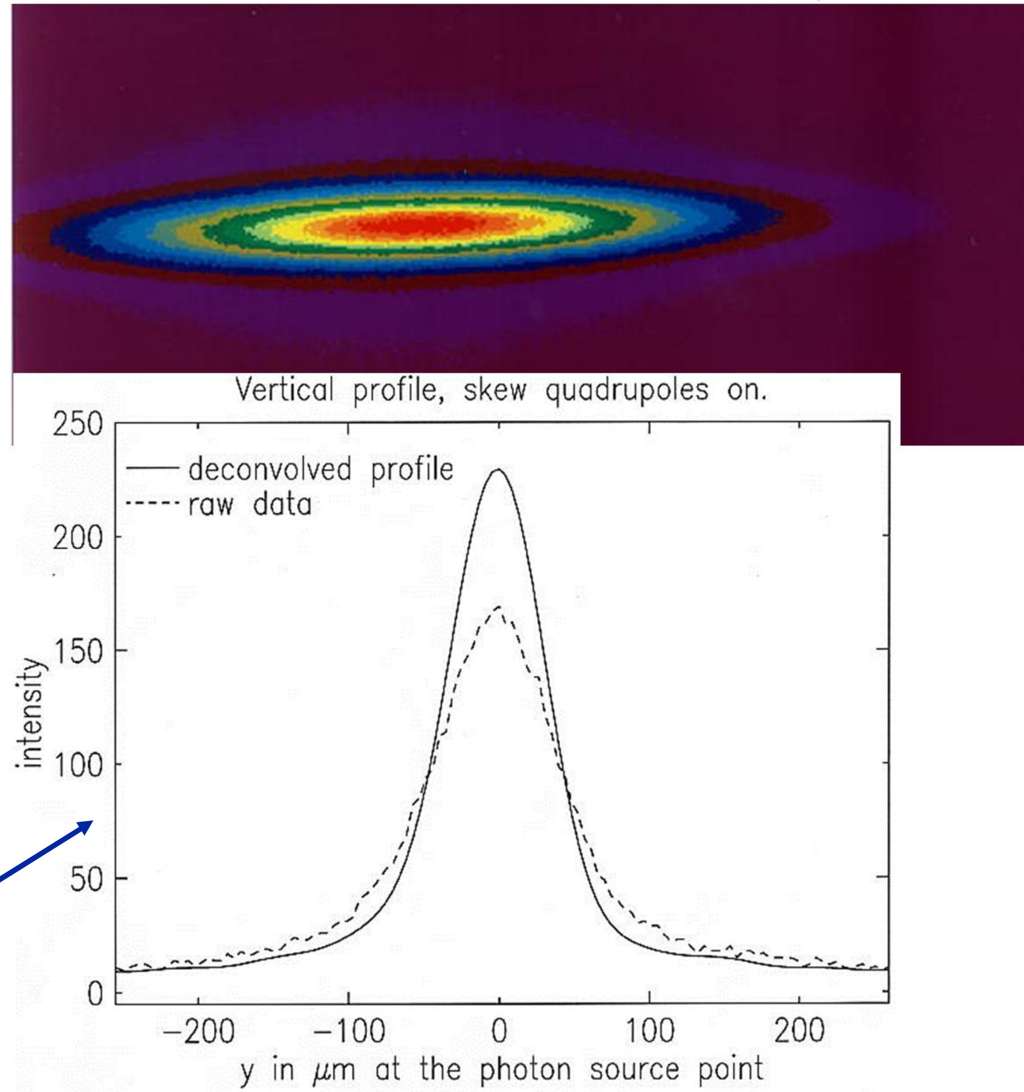

Diffraction

Even though we are dealing with X-Rays, diffraction is a significant resolution limitation. The diffraction pattern was calculated numerically as a function of pinhole dimension. For large pinholes, it looks like a geometric image of the square pinhole. For small pinholes, it looks like Fraunhofer diffraction, getting larger as the pinhole gets smaller. The pinhole size that gives the best resolution is somewhere between the Fraunhofer regime and geometric image.

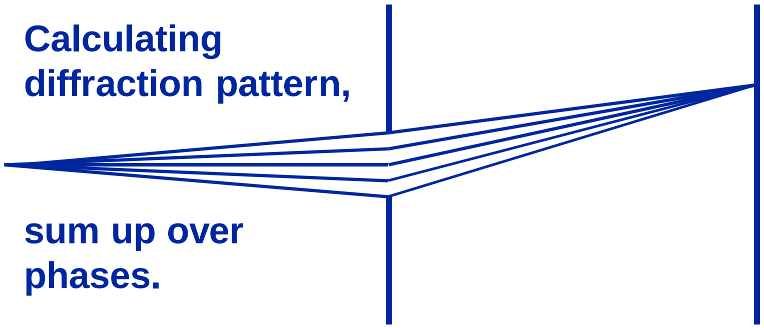

The diffraction pattern must be integrated over the spectrum absorbed by the YAG phosphor.

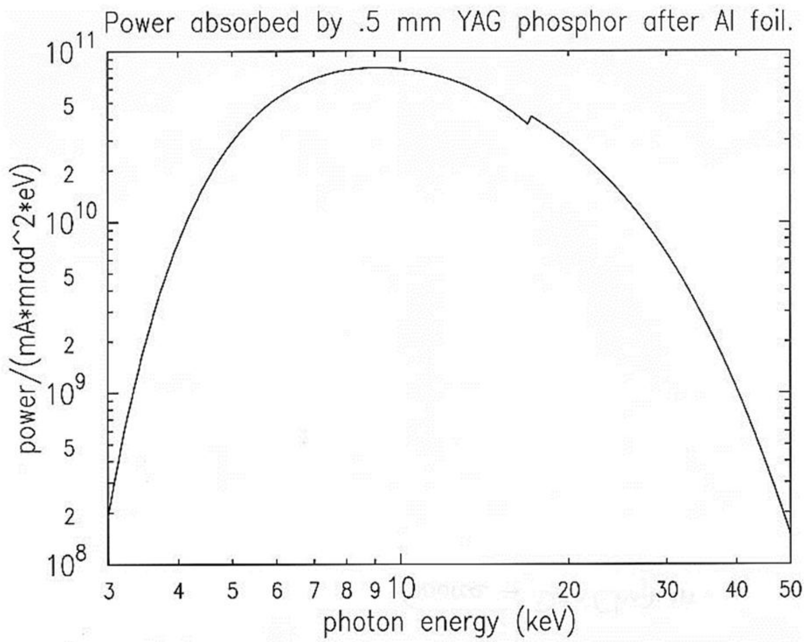

Resolution functions

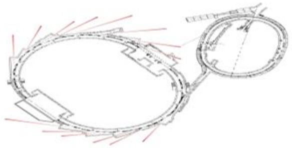

All secondary maxima in the diffraction pattern wash out when integrating over the wavelength spectrum.

The resolution of the detector was measured by placing a very narrow slit just in front of the phosphor.

The measured image is a convolution of the real profile with the resolution functions.

$$I_{\text{meas}} = R \otimes I_{\text{real}}$$

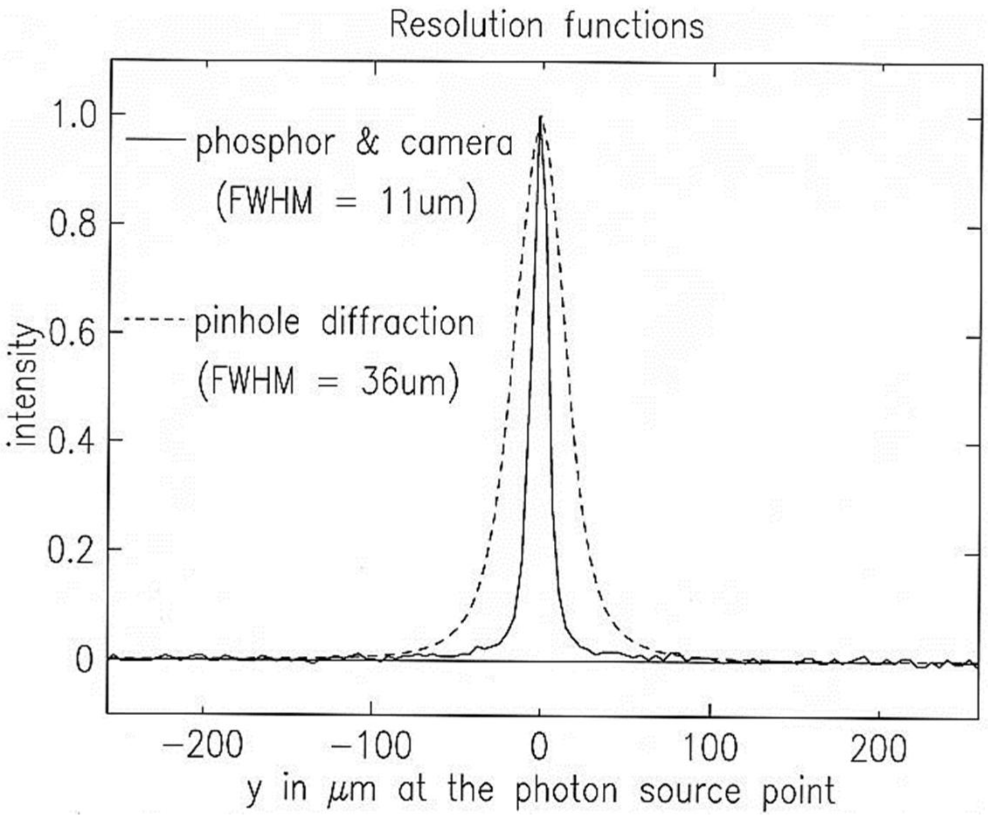

The data and resolution functions are sets of discreet points, so the deconvolution could be turned into a big matrix inversion. A more traditional method uses FFTs. Convolution in frequency space is simply multiplication, so deconvolution becomes division.

Deconvolution

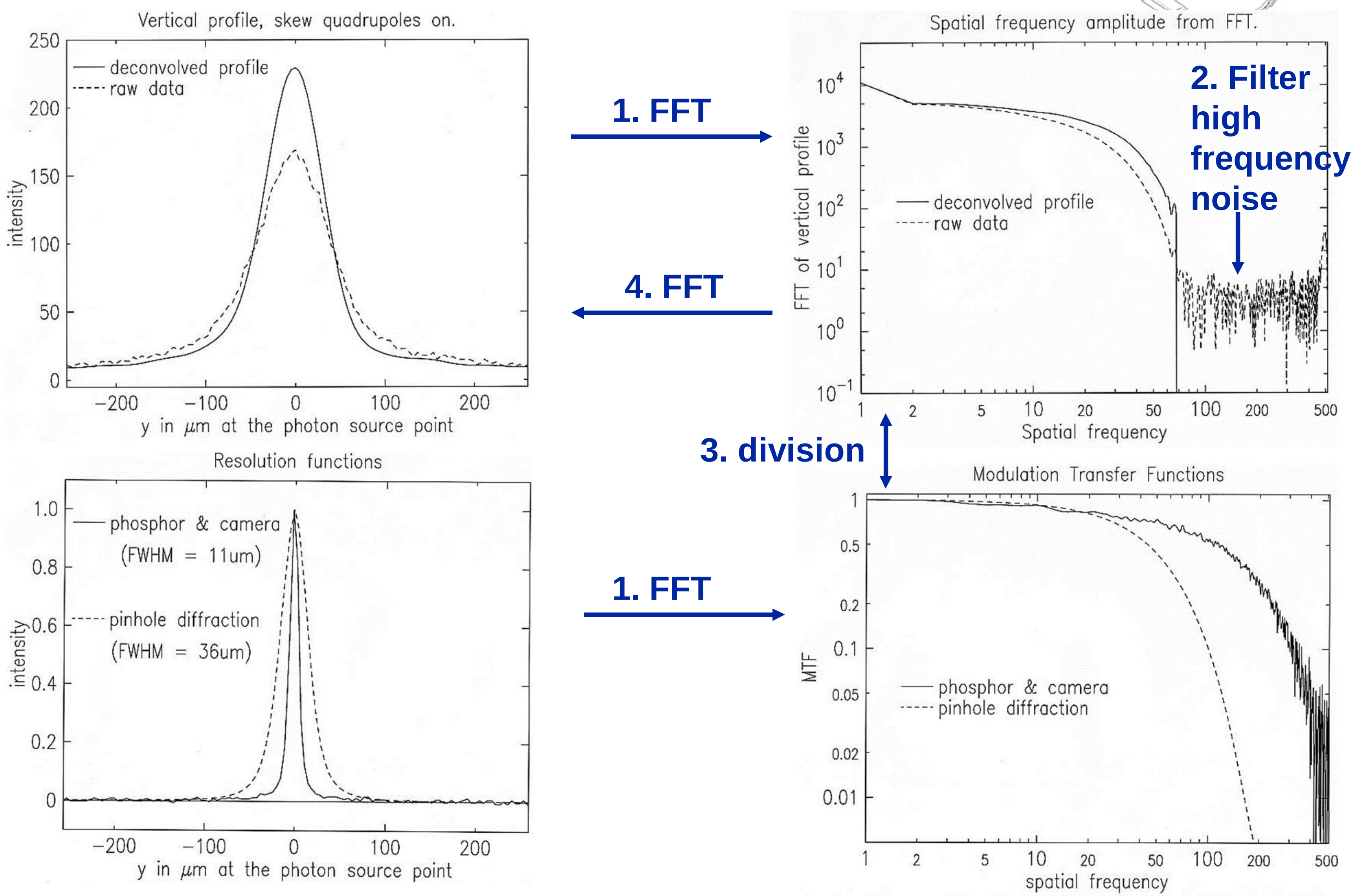

Modulation transfer function

Instead of dividing FFTs, use only amplitude part of FFT – called modulation transfer function (MTF).

MTF is a common way to specify resolution. For example, this graph came with the video camera that was used for the X-Ray Ring pinhole camera.

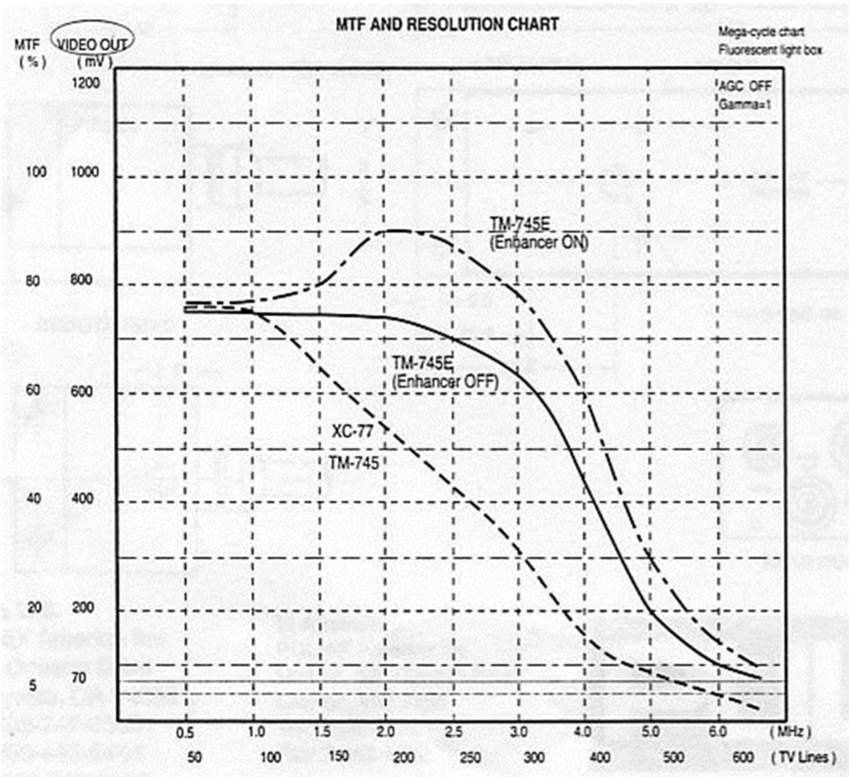

Pulnix video camera MTF

Numerical Recipes, Cambridge Press, is a good reference for FFTs and deconvolution.